ISSN (Print) 1226-1750
ISSN (Online) 2233-6656
Journal of Magnetics 25(4), 674-680 (2020) https://doi.org/10.4283/JMAG.2020.25.4.674

Evaluation of CT Imaging Characteristics and Effect of CTDI Phantom Size on Contrast Materials

Pil-Hyun Jeon[1] and Cheol-Ha Baek[2]*

[1]*Department of Radiology, Yonsei University, Wonju Severance Christian Hospital, Gangwon 26426, Republic of Korea*
[2]*Department of Radiological Science, Kangwon National University, Gangwon 25949, Republic of Korea*

(Received 27 October 2020, Received in final form 13 December 2020, Accepted 14 December 2020)

Recently, there have been several physics and clinical studies on the use of lower tube potentials in CT imaging, with the purpose of improving image quality or further reducing radiation dose. We investigated an experimental study using a series of different sized, polymethyl methacrylate (PMMA) phantoms, demonstrating the potential strategy for dose reduction and to distinguish component of plaque by imaging their energy responses using CT. We investigated the relationship between different sizes of cylinderic PMMA equivalent phantoms with diameter of 12, 16, 20, 24, and 32 cm and used contrast at various tube voltages (80, 100, 120, and 140 kVp) using a 16–detector row CT scanner. The contrast represented CT numbers as different materials for the water, calcium chloride, and iodine. Phantom insertions also allow quantitative measures of image noise, contrast, contrast-to-noise ratio (CNR) and figure of merit (FOM). When evaluating FOM, it was found that the lower kVp provided the better CNR. An experimental study was performed to demonstrate reduced dose for both dose efficient and practical feasibility for different patient sizes and diagnostic tasks by relating achievable CNR and the volume CT dose index (CTDI vol). The use of spectra optimized to the specific application could provide further improvements of distinguishing iodine, calcium and plaque component for patient size. The purpose of this study was to evaluate variations in image noise and contrast using different tube potentials in a CTDI phantom on contrast imaging.

Keywords : computed tomography, Image characteristics, CTDI phantom, tube voltage

1. Introduction

One of the major challenges with the use of computed tomography (CT) is to establish the proper tradeoff between radiation dose and image quality [1, 2]. Spectral optimization has not been a topic of great concern; high tube voltages around 120 kV have been in use since the beginning of CT [3]. Improved acquisition protocols with tube potentials of about 80 kVp for imaging iodine have been proposed for diagnostic CT imaging in a previous study that included children and adults. Increased X-ray attenuation results in reduced detector exposure thereby increasing image noise. When patient size is above a particular threshold for small FOV (field of view), the benefit of improved contrast enhancement is negated by the increased noise level, and the lower tube potential may reduce image quality compared to a higher tube potential at the same dose. For example, if CT examinations can be performed at different tube potentials and achieve comparable image quality, then it is clearly desirable to select the technique that minimizes patient dose. A certain amount of photons has to pass through the patient and be captured by detectors. Increased beam hardening in large patients will increase the mean photon energy and reduce image contrast [4, 5]. However, with improved X-ray penetration, differential attenuation decreases and so does the contrast between soft tissues and materials with high atomic numbers, such as bones and iodine. A more recent study used a dose-normalized contrast-to-noise ratio as the criterion to determine the optimal tube potential and thereby quantify its dependence on phantom sizes and contrast material [6-9]. Their results demonstrated that the selection of tube potential has to be adapted to the size of the patient and to the diagnostic task to a much greater degree than is common practice today. In this work, we directly quantified the relative dose that is required at each tube potential to achieve a target image quality. In our phantom study, we investigated the contrast-

*Corresponding author: Tel: +82-33-540-3384
Fax: +82-33-540-3389, e-mail: baekch@kangwon.ac.kr

to-noise ratio (CNR) and figure of merit (FOM) relating to the CNR-to-dose ratio for different concentrations of iodine, calcium chloride, water, and fat inserts in different polymethyl-methacrylate (PMMA) phantom backgrounds. Image CNR characteristics were studied for the range of lesion composition of interest in CT, which ranged from low Z (i.e., fat) to high Z (i.e., iodine) materials. The weighted computed tomography dose index ($CTDI_w$) for the protocol setting was measured to compare changes in image quality at the same X-ray dose. The purpose of this study was to evaluate variations in image noise and contrast using different tube potentials in a CTDI phantom on contrast imaging.

2. Materials and Methods

2.1. Geometry and dimensions of phantoms

The PMMA phantoms used for image quality and dose measurements are shown with the CT units in the table. We investigated the relationship between different sizes of five cylindrical 150-mm long PMMA-equivalent phantoms with diameters of 12, 16, 20, 24, and 32 cm, as shown in Fig. 1. Figure 1(b) shows the scout views with different sizes of PMMA phantoms.

Each phantom had five holes (one central and four peripheral holes, size 13 mm^2) in Fig. 2.

The positions of a circular region of interest (ROI) with the material (center) and the background (peripheral) for contrast, noise, CNR, and FOM are shown in Fig. 3.

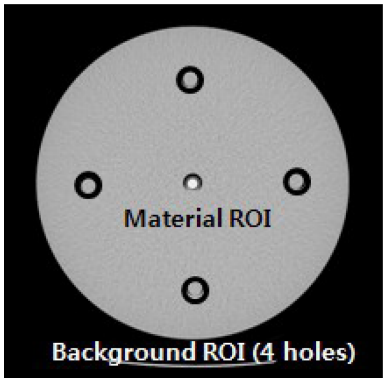

Fig. 3. Positions of the circular ROI with the material (center) and the background (peripheral) for contrast, noise, CNR, and FOM.

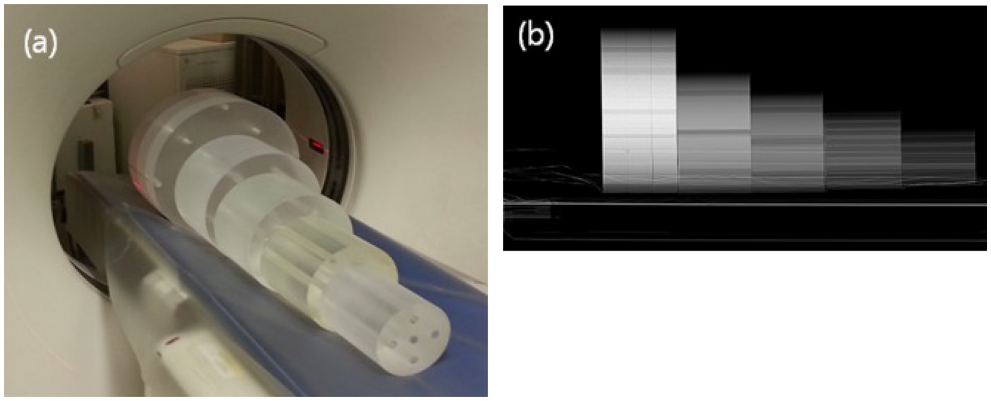

Fig. 1. (Color online) (a) PMMA phantoms used for image quality and dose measurements. A cylindrical PMMA phantom (12, 16, 20, 24, and 32 cm in diameter) was installed. (b) CT scout view with different sizes of PMMA phantom.

Fig. 2. (Color online) PMMA phantom used for measurements and plastic tube inserted containing water (0 HU), iodine (200 HU), $CaCl_2$ (1000 HU), and fat (-120 HU) contrast solutions.

Table 1. Radiation dose summary for the CT scan used in this study. Tube current settings were as close as possible to 10 mGy for the four tube potentials.

kVp	mAs				
	12 cm	16 cm	20 cm	24 cm	32 cm
80	130	200	210	300	330
100	70	105	110	155	195
120	50	70	70	95	125
140	35	50	50	65	85

As in shown in Fig. 2, several samples were placed in the central region of the phantoms to allow measurements of water, iodine, calcium, and fat signals within a given PMMA background. The calcium chloride and iodine were dissolved in water to mimic corresponding concentrations. The calcium chloride concentration was 600 mg/mL for $CaCO_3$, and the iodine concentrations were 1.8 mg/mL and 370 mgI/mL for iodine Pamiray (Dong Kuk, Seoul, Korea).

2.2. CT protocol

Light Speed 16-slice CT (GE, Milwaukee, WI, USA) was used for evaluation of the radiation dose. Image noise and contrast were evaluated as measures of image quality. CT scanning of the PMMA phantoms was performed with four tube potentials: 80, 120, 100, and 140 kVp and with a tube current of 30 to 330 mAs, respectively, as shown in Table 1.

We performed the effective tube current settings so that the phantom volume CT dose index ($CTDI_{vol}$) was as close as possible to 10 mGy for the four tube potentials.

2.3. Radiation dose measurement for experiments

CTDI has dominated CT dosimetry for more than 25 years since it allows quality assurance and radiation dose optimization in CT imaging. Standard CTDI measurements were universally adopted and routinely performed at the periphery, i.e. 1 cm below the surface ($CTDI_p$) and at the center ($CTDI_c$) of the standard head and body PMMA cylindrical phantoms using a pencil ionization chamber with an active length of 100 mm. In this study, dose estimates were obtained by standard measurements, using ionization chambers to measure the CTDI with a 10-cm pencil-shaped ion chamber and an Unfors Xi CT Electrometer (Unfors Xi Corp., Billdal, Sweden). The weighted value of CTDI was defined as follows:

$$CTDI_w = 1/3\,CTDI_{100c} + 2/3\,CTDI_{100p} \quad (1)$$

Table 2. Imaging parameter and image quality results of water, iodine, calcium chloride, and olive oil samples in the plastic tube at 80, 100, 120, and 140 kVp with a PMMA background.

kVp	Contrast		Noise		CNR		FOM	
	12 cm	32 cm	12 cm	32 cm	12 cm	32 cm	12 cm	32 cm
Water (0 HU)								
80	3.8	1.6	2.5	34.7	21.1	2.4	5.1	0.1
100	0.1	1.6	2.2	23.6	26.9	3.5	4.9	1.0
120	0.1	8.3	1.8	18.1	36.5	4.7	5.3	1.1
140	0.2	8.3	1.3	15.0	49.4	5.9	6.2	1.2
Iodine 1.8 mg/mL (200 HU)								
80	326	256	4.4	29.3	42.0	3.6	10.2	1.5
100	260	199	3.2	27.2	33.8	2.0	6.1	0.6
120	210	157	2.6	24.6	25.7	0.8	3.8	0.2
140	178	136	2.1	12.9	21.1	0.1	2.6	0.0
Bone/Calcium chloride 600 mg/mL (1000 HU)								
80	1334	1035	5.1	53.5	198	48.9	55.5	6.9
100	1053	804	3.2	33.0	201	38.0	38.0	4.7
120	870	633	2.0	21.6	210	33.3	29.4	3.5
140	746	520	2.4	19.6	228	22.8	24.8	2.9
Fat/Olive oil (-120 HU)								
80	-155	-127	4.2	24.7	43.1	6.3	10.5	2.4
100	-138	-109	3.0	22.4	52.3	7.2	9.4	2.1
120	-128	-97	4.3	18.1	64.0	8.1	9.3	1.9
140	-120	-96	3.2	18.7	81.2	10.0	10.1	1.9

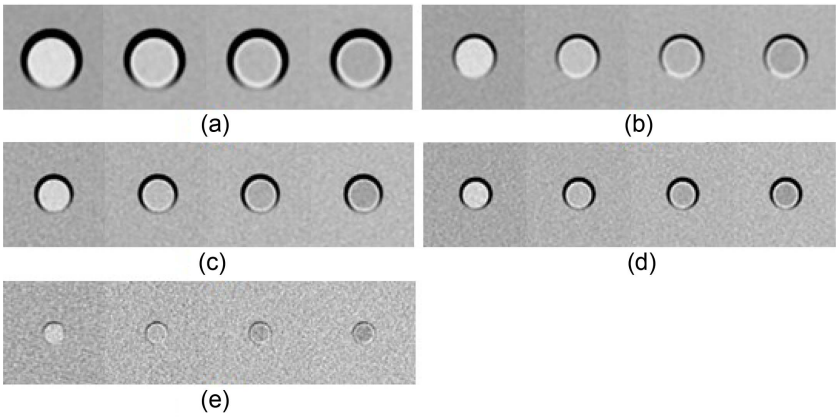

Fig. 4. Comparison ROI of acquired PMMA phantom images with different tube potentials: (a) 12 cm (b) 16 cm (c) 20 cm (d) 24 cm (e) 32 cm PMMA phantom at 80, 120, 100, and 140 kVp from left to right, respectively.

2.4. Image quality metrics

The variables used to determine the efficiency of the phantom were contrast, noise, CNR, $CTDI_{vol}$, and a figure of merit (FOM) relating CNR and dose. The CNR was expressed as:

$$CNR = \frac{{}_{EMBED}\left|\bar{P}_{ROI\ material} - \bar{P}_{ROI\ background}\right|}{{}_{EMBED}\sqrt{\sigma^2 ROI\ material + \sigma^2 ROI\ background}} \quad (2)$$

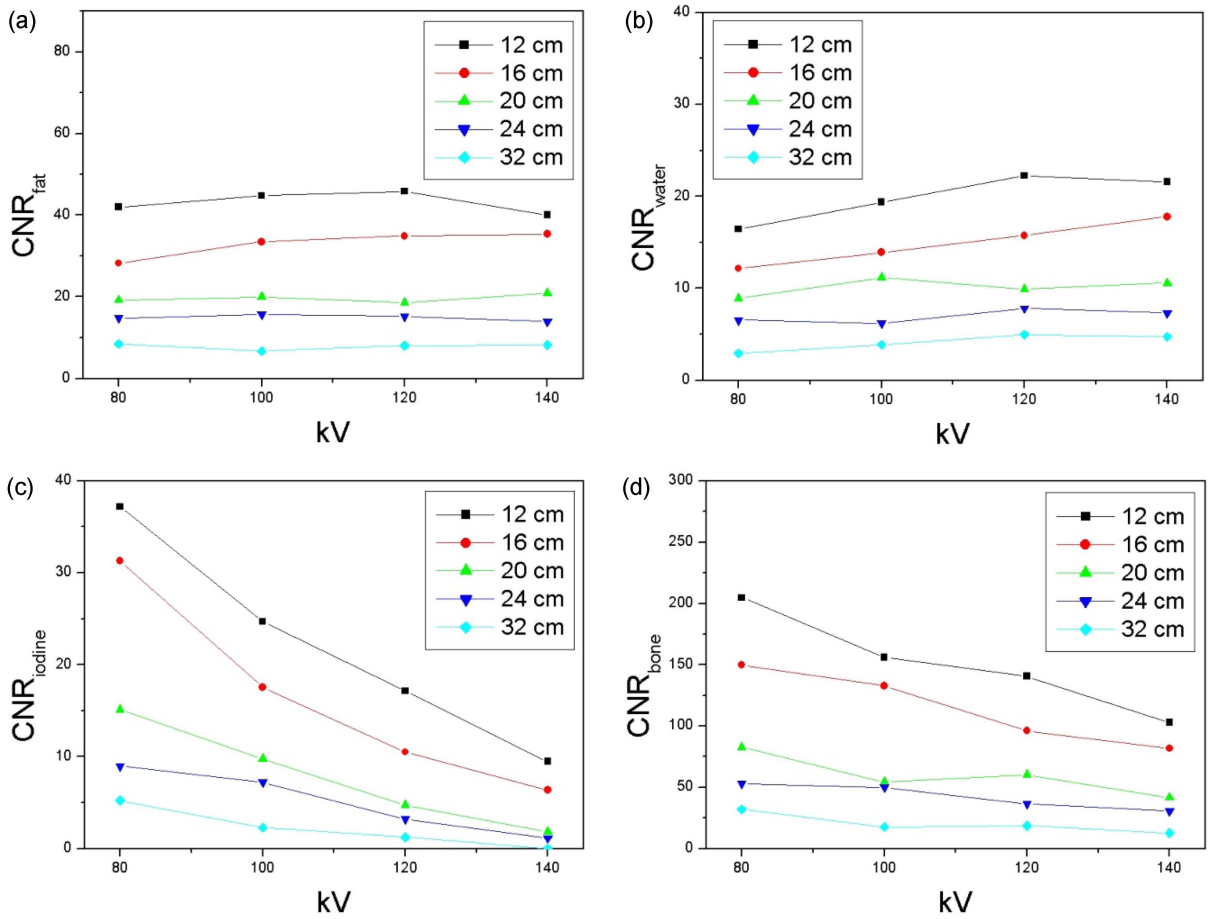

Fig. 5. (Color online) CNR values as a function of tube potential for 12 cm to 32 cm PMMA phantoms for (a) fat, (b) water, (c) iodine, and (d) bone.

Where $P_{ROI\ material}$ is the average signal value in Hounsfield units (HU) inside the water, fat, iodine, and calcium chloride plastic tube under consideration, and $\sigma_{ROI\ material}$ and $\sigma_{ROI\ background}$ are the corresponding standard deviations. $P_{ROI\ background}$ is the averaged signal in the PMMA background. The radiation exposure was quantified by the $CTDI_{vol}$. To better discern the effect of tube potential and phantom size on CNR in relation to patient exposure, a FOM was calculated as follows:

$$FOM = \frac{CNR}{\sqrt{CTDI_{vol}}} \quad (3)$$

FOM is independent of exposure and can be used as a measure of improvement in image quality per radiation dose. Therefore the assessment of image quality with regard to dose minimization is carried out using a FOM.

3. Results

3.1. Image contrast and noise for each phantom size

Increasing the tube potential from 80 to 140 kVp changed the water from –1.2 to 7.0 HU, bone from 1334 to 520 HU, iodine from 326 to 136 HU, fat from –151 to –96 HU, and PMMA for background from 88 to 113 HU. Fig. 4 shows how lesion contrast changed with the selected tube potential for iodine.

3.2. Image quality metrics for CNR

As expected, image noise; contrast; and the corresponding CNR, $CTDI_{vol}$, and FOM were affected by the acquisition tube potential parameters. A full summary of these results are shown in Table 2.

With low kVp, contrast increased but image noise also increased, as shown in Fig. 4.

However, Fig. 5 provides a comparison of how much CNR one gains per unit dose. This gain increases exponentially at higher CNR values, as shown in Fig. 6. The graph demonstrates a dose reduction of 50 % with the use of 80 kVp instead of 140 kVp.

Our analysis also allows for an assessment of the overall effect of phantom diameter on dose image quality, with a statistically significant increase in $CTDI_{vol}$ ($p < 0.0001$) and a statistically significant decrease in image quality ($p < 0.0001$ for CNR) with increasing phantom

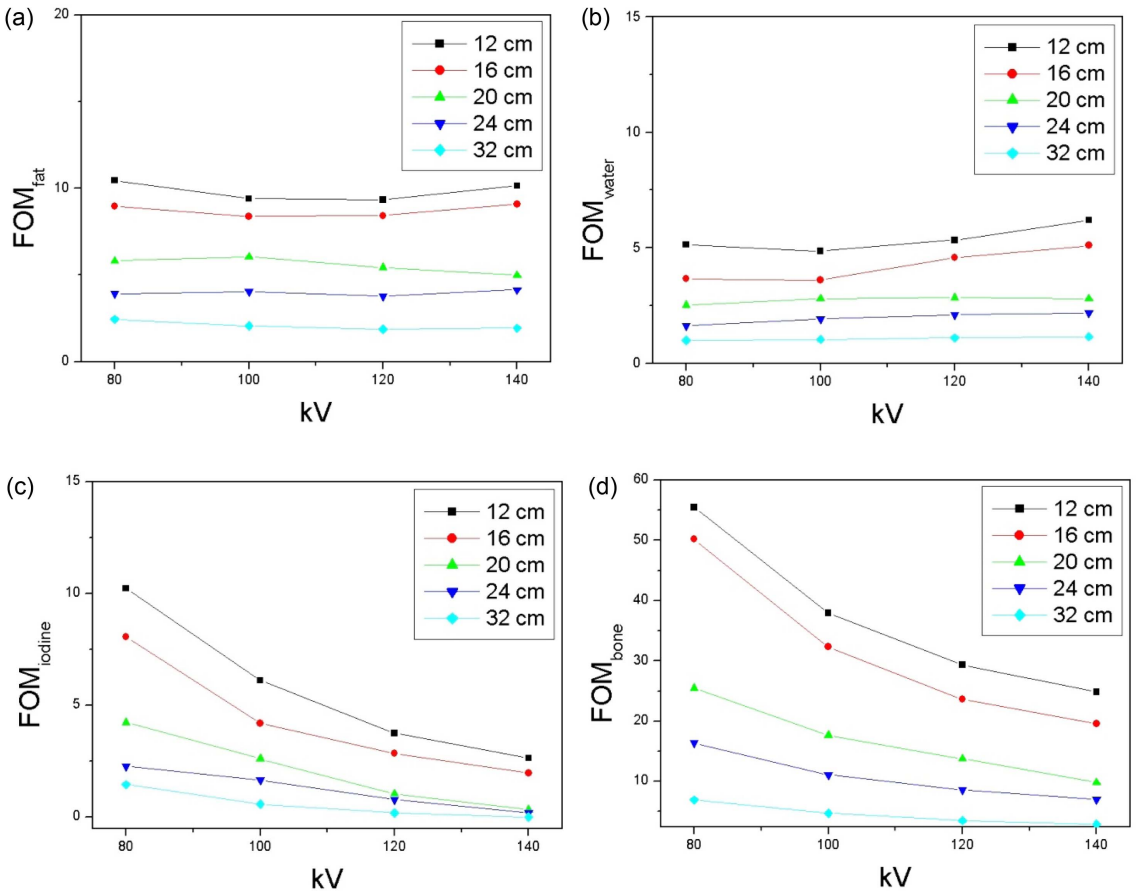

Fig. 6. (Color online) FOM values as a function of tube potential for 12 cm to 32 cm PMMA phantoms for (a) fat, (b) water, (c) iodine, and (d) bone.

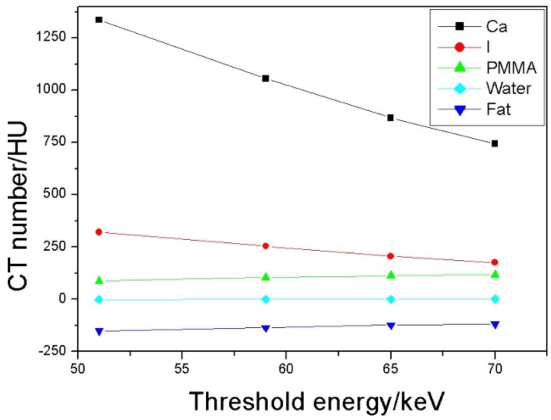

Fig. 7. (Color online) A plot of CT values for different materials in a phantom evaluated at 80, 100, 120, and 140 kVp.

size (Table 2 and Fig. 5).

3.3. Effect on FOM

The FOM enabled evaluation of the effect of varying tube voltage settings on CNRs since this difference prevented direct comparisons of image quality characteristics of different tube potentials. The FOM was improved with the use of lower kVp (80 kVp) for both calcium and iodine (Fig. 6). Additionally, the relationship between the FOM and different CT energies for calcium and iodine are shown in Fig. 6.

4. Discussion

Different size phantoms are compatible with CT and allow quantitative comparisons of important performance metrics, such as image noise, contrast, CNR, and radiation exposure. The phantom allows flexible selection of materials to be inserted. We used water, olive oil for fat, iodinated contrast material, and calcium chloride for bone to establish the relationship between the material concentration and CT attenuation. This result was consistent at different tube potentials (80, 100, 120, and 140 kVp). Image noise is closely related to tube potential and tube current, and both of these parameters determine photon fluency and incident beam. In order to compensate for image noise when decreasing the tube potential, the tube current must increase [10, 11]. A higher tube potential could increase the radiation dose as a result of exposure to higher X-ray energies. Therefore, selection of the appropriate scanning parameters is critical to obtaining optimum image quality as well as minimizing radiation exposure. Scanning with lower tube potential results in increased noise caused by direct reduction in photon flux. Lower tube potential scans have as smaller number of photons striking the detector, which results in limited data to construct an optimal image. Inadequate amounts of constructed data may cause the image appearance to be very grainy and influence the diagnostic value of the images. There is a subtle decreasing pattern, which might be due to insufficient tube current compensation. Our findings are consistent with a previous study which the CT attenuation value of iodine increased at a lower tube potential and resulted in higher image enhancement [12-18]. A potential explanation for this phenomenon is the photoelectric effect. At a lower tube potential, the influence of photoelectric interactions in the presence of iodinated contrast media is greater compared with Compton scattering effects because of the 33 keV k-edge of iodine [10, 11]. As a consequence, there is a much more dramatic increase in the linear attenuation coefficient of iodine than for water and fat. The increased image noise significantly reduces conspicuity of low contrast lesions, where the low kVp may diminish CNR. For imaging materials of higher atomic number Z, such as contrast media, calcifications, and the skeleton, lower tube potentials appear

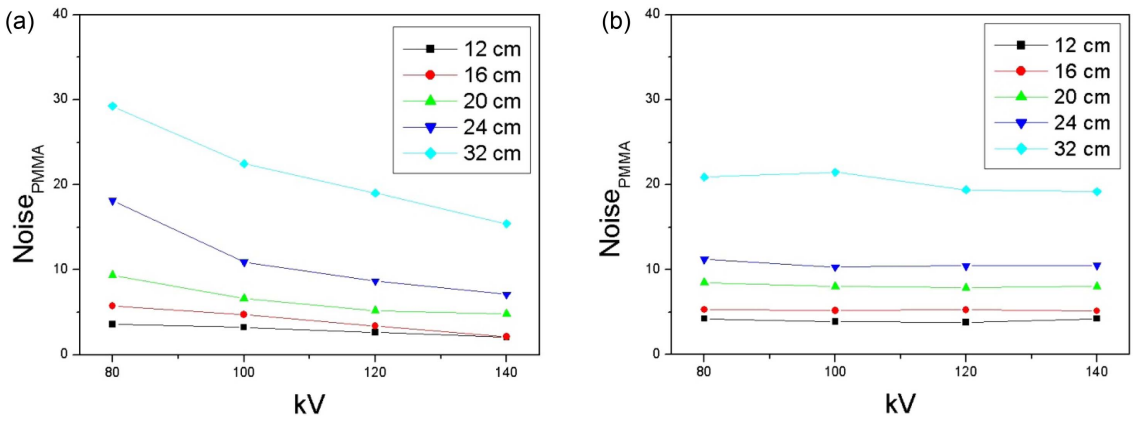

Fig. 8. (Color online) Noise values as a function of tube potential for 12 cm to 32 cm PMMA phantoms at fixed 200 mAs and the 10 mGy $CTDI_{vol}$.

appropriate. The representative photon energies are 51 keV at 80 kVp, 59 keV at 100 kVp, 65 keV at 120 kVp, and 70 keV at 140 kVp [12]. The reduction of lesion contrast relative to water is greatest for high atomic number materials, such as iodine (Z=53) and bone (Z= 20), and low atomic number materials, such as water (Z=7.51) and fat (Z=6.46), as shown in Fig. 7.

The CT number for calcium solution declined as energy increased, whereas the CT number of oil increased. Contrast increased strongly for lower energies. Noise increased similarly for lower energies and a given object size. Of greatest importance, however, is that a simple CNR of image quality only correlates with imaging performance when lesions are embedded in a uniform background. The same radiation dose (10 mGy) can be adjusted according to the constraint noise level for various sizes of a PMMA background at different tube potentials, as shown in Fig. 8.

Plotting CNR/$CTDI_{vol}$ as figure of merit against beam energy revealed interesting results. CNR measures image quality, whereas FOM quantifies improvements in image quality per exposure risk to the patient. This study compared the image quality acquired for different patient sizes, contrast materials, tube potentials, and dose settings and may lead to a strategy to improve image quality using the reference tube potential and dose settings.

5. Conclusion

This paper presents to evaluate variations in image noise and contrast using different tube potentials in a CTDI phantom on CT imaging. We performed a study to demonstrate reduced dose efficiency and practical feasibility for different patient sizes and diagnostic tasks by relating achievable CNR and $CTDI_{vol}$. Our results support using lower kVp scan protocols in contrast imaging. There is a clear differentiation between imaging of density-dependent contrasts and of contrasts presented by high-Z materials. The use of spectra optimized to the specific application could provide further improvements in distinguishing iodine, calcium, and plaque componentsbased on patient size. Our analysis of phantom CT scans revealed comparable image quality, and indicates that the phantom size significantly affects the radiation dose in clinical CT studies.

References

[1] W. A. Kalender, P. Deak, M. Kellermeier, M. Straten, and S. V. Vollmar, Med. Phys. **36**, 993 (2009).
[2] S. V. Vollmar and W. A. Kalender, Br. J. Radiol. **82**, 920 (2009).
[3] H. J. Brisse, J. Brenot, N. Pierrat, G. Gaboriaud, A. Savignoni, Y. De Rycke, S. Neuenschwander, B. Aubert, and J. Rosenwald, Phys. Med. Biol. **54**, 1871 (2009).
[4] H. J. Brisse, L. Madec, G. Gaboriaud, T. Lemoine, A. Savignoni, B. Aubert, and J. C. Rosenwald, Med. Phys. **34**, 3018 (2007).
[5] W. Huda, K. A. Lieberman, J. Chang, and M. L. Roskopf, Med. Phys. **31**, 595 (2004).
[6] R. Francis, D. Lepori, P. Monnin, J. F. Valley, P. Schnyder, and F. Gudinchet, Eur. Radiol. **14**, 835 (2004).
[7] W. Huda, Pediatr, Radiol. **32**, 709 (2002).
[8] W. Huda, K. M. Ogden, and M. R. Khorasani, Phys. Med. Biol. **53**, 4719 (2008).
[9] E. L. Nickoloff, A. K. Dutta, and Z. F. Lu, Med. Phys. **30**, 395 (2003).
[10] L. Yu, H. Li, J. G. Fletcher, and C. H. McCollough, Med. Phys. **37**, 234 (2010).
[11] S. P. Kalva, D. V. Sahani, F. Piter, and S. Sanay, J. Comput. Assist. Tomogr. **30**, 391 (2006).
[12] J. E. Ngaile, P. Msaki, and R. Kazema, Radiat, Prot. Dosim. **148**, 189 (2012).
[13] M. J. Siegel, B. Schmidt, C. Suess, and C. Hildebolt, Radiology **233**, 515 (2004).
[14] R. Brooks and G. D. Chiro, Med. Phys. **3**, 237 (1976).
[15] W. A. Kalender, S. Buchenau, P. Deak, M. Kellermeier, O. Langner, M. Straten, S. Vollmar, and S. Wilharm, Med. Phys. **24**, 71 (2008).
[16] M. K. Kalra, M. M. Maher, T. L. Toth, B. Schmidt, B. L. Westerman, H. T. Morgan, and S. Saini, Radiology **230**, 619 (2004).
[17] C. M. Chen, S. Y. Chu, and M. Y. Hsn, Eur. Radiol. **24**, 460 (2014).
[18] T. Yoshi, K. Miwa, M. Yamaguchi, et al., EJNMMI Physics **7**, 56 (2020).